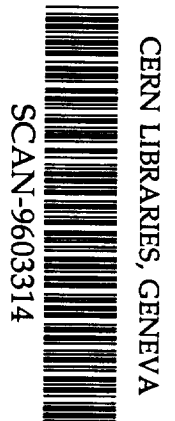


Direct  $\omega \rightarrow \pi^+ + \pi^-$  Decay in the Analysis of Rho-Omega Mixing

C.M. Shakin and Wei-Dong Sun

Department of Physics and Center for Nuclear Theory  
Brooklyn College of the City University of New York  
Brooklyn, New York 11210



*Scw 96/14*

(March, 1996)

Submitted to Physical Review D

## Abstract

It has recently been shown that it is not possible to obtain a model independent value of the matrix element describing rho-omega mixing,  $\langle \rho^0 | H_{SB} | \omega \rangle$ , from the study of the pion electromagnetic form factor without knowledge of the amplitude for direct omega decay  $\omega \rightarrow \pi^+ + \pi^-$ . In this work we calculate the amplitude for direct omega decay in a generalized Nambu–Jona-Lasinio model. We find that that amplitude is quite small. We perform an analysis of the pion form factor and extract a value for  $\langle \rho^0 | H_{SB} | \omega \rangle$ . In our model, that matrix element is directly related to the difference of the current masses of the up and down quarks. Our analysis suggests values for the current quark masses of  $m_u^0 \simeq 4$  MeV and  $m_d^0 \simeq 7$  MeV, with  $\Delta m = m_d^0 - m_u^0 \simeq 3$  MeV.

## I. Introduction

In a previous work [1] we provided a foundation for the vector meson dominance (VMD) model of electromagnetic form factors making use of an extended version of the Nambu–Jona-Lasinio (NJL) model [2,3]. We studied the pion electromagnetic form factor and included the effect of rho-omega mixing [4]. One of the goals of such studies is to extract a value for the matrix element,  $\langle \rho^0 | H_{SB} | \omega \rangle$ , that governs the strength of rho-omega mixing. In early work, values of  $\langle \rho^0 | H_{SB} | \omega \rangle = -(4520 \pm 600) \text{ MeV}^2$  were found [5]. Since there is a known electromagnetic contribution, the strong interaction matrix element is then  $\langle \rho^0 | H_{SB}^{st} | \omega \rangle = -(5153 \pm 600) \text{ MeV}^2$ . This value may be used to determine the difference of the up and down current quark masses,  $\Delta m = m_d^0 - m_u^0$ , using our extended NJL model [1,6]. (Note that the value of the matrix element obtained from fitting data depends upon the values used for the meson decay constants in the theoretical analysis.)

Recently, it was shown that one cannot determine  $\langle \rho^0 | H_{SB} | \omega \rangle$  in a model-independent fashion, since the contribution of direct omega decay is unknown [7]. (Direct omega decay is defined as the amplitude for  $\omega \rightarrow \pi^+ + \pi^-$  that does not proceed via  $\rho$ - $\omega$  mixing.) It is clear that a model of direct omega decay will be useful in understanding the importance of that amplitude in the analysis of rho-omega mixing. In this work we will extend our (microscopic) version of the VMD model to include direct omega decay in a new analysis of the pion electromagnetic form factor.

The organization of our work is as follows. In Section II we review various relations that appear in a momentum-space bosonization of our version of the NJL model which includes a description of confinement [2,3]. In Section III we see how the various tensors defined in

Section II may be used to provide a basis for the VMD model. We then discuss the pion electromagnetic form factor. One new feature of our analysis is the appearance of momentum-dependent meson decay "constants" and momentum-dependent meson-quark coupling "constants". We also provide an expression for  $\langle \rho^0 | H_{SB}^{st} | \omega \rangle$  in terms of quantities that may be calculated in our model. In Section IV we present a calculation of the momentum-dependent coupling constants,  $g_{\rho\pi\pi}(q^2)$  and  $g_{\omega\pi\pi}(q^2)$  and, in Section V, we present numerical results for the pion electromagnetic form factor, including the effect of direct omega decay. Within the context of our model, that effect is seen to be quite small. Therefore, we are able to determine values for  $\langle \rho^0 | H_{SB} | \omega \rangle$  that lead to reasonably good fits to the experimental data [8]. Finally, Section VI includes some further discussion and conclusions.

## II. Momentum-Space Bosonization of an Extended Nambu–Jona-Lasinio Model

In this section we review various relations that may be used to provide a microscopic basis for the VMD model [1]. We make use of a version of the NJL model that we have developed and which includes a description of confinement [2,3].

With reference to Fig. 1, it is useful to define a number of tensors [2]

$$\hat{J}_{(\rho)}^{\mu\nu}(q) = -\bar{g}^{\mu\nu}(q) \hat{J}_{(\omega)}(q^2) \quad , \quad (2.1)$$

$$\hat{J}_{(\omega)}^{\mu\nu}(q) = -\bar{g}^{\mu\nu}(q) \hat{J}_{(\omega)}(q^2) \quad , \quad (2.2)$$

$$\hat{K}_{(\rho)}^{\mu\nu}(q) = -\bar{g}^{\mu\nu}(q) \hat{K}_{(\rho)}(q^2) \quad , \quad (2.3)$$

$$\hat{K}_{(\omega)}^{\mu\nu}(q) = -\bar{g}^{\mu\nu}(q) \hat{K}_{(\omega)}(q^2) \quad , \quad (2.4)$$

and

$$\hat{J}_{(\omega\rho)}^{\mu\nu}(q) = -\bar{g}^{\mu\nu}(q) \hat{J}_{(\omega\rho)}(q^2) \quad , \quad (2.5)$$

with  $\bar{g}^{\mu\nu}(q) \equiv g^{\mu\nu} - q^\mu q^\nu / q^2$ . The tensors  $\hat{J}^{\mu\nu}(q)$  are obtained from the basic quark-antiquark loop integrals of the NJL model when we include a vertex function (the shaded triangular area in Fig. 1) that implements our model of confinement [2,3]. We note that, if the current quark masses,  $m_d^0$  and  $m_u^0$ , are equal, we have  $\hat{J}_{(\rho)}^{\mu\nu}(q) = \hat{J}_{(\omega)}^{\mu\nu}(q)$ .

The tensor  $\hat{K}_{(\rho)}^{\mu\nu}(q)$  describes the coupling of quark-antiquark states to the two-pion continuum [2], while the main contribution to  $\hat{K}_{(\omega)}^{\mu\nu}(q)$  arises from coupling of the  $q\bar{q}$  states to the three-pion continuum. (Note that  $K_{(\omega)}(q^2) \ll K_{(\rho)}(q^2)$ .)

The tensor  $\hat{J}_{(\rho\omega)}^{\mu\nu}(q)$  describes the coupling between states of the rho and omega due to the fact that  $m_d^0 \neq m_u^0$  [6]. It may be calculated by considering the loop integral for either the up or the down quark and then taking the difference, as is indicated in a schematic fashion in Fig. 1c. Values of  $\hat{J}_{(\rho\omega)}(q^2)$ , obtained in that manner, are presented in Ref. [6].

We may define a  $T$  matrix for  $q\bar{q}$  scattering by summing a series of diagrams whose values are represented by  $q\bar{q}$  loop integrals. The result may be written in terms of the coupling

constants of the model and the functions defined in Eqs. (2.1)-(2.4). Our Lagrangian is

$$\begin{aligned}
\mathcal{L}(x) = & \bar{q}(x)(i\partial - m_q^0)q(x) \\
& + \frac{G_S}{2} \left[ (\bar{q}(x)q(x))^2 + (\bar{q}(x)i\gamma_5\bar{\tau}q(x))^2 \right] \\
& - \frac{G_\rho}{2} \left[ (\bar{q}(x)\gamma^\mu\bar{\tau}q(x))^2 + (\bar{q}(x)\gamma_5\gamma_\mu\bar{\tau}q(x))^2 \right] \\
& - \frac{G_\omega}{2} (\bar{q}(x)\gamma^\mu q(x))^2 + \mathcal{L}_{conf}(x) \quad ,
\end{aligned} \tag{2.6}$$

where  $\mathcal{L}_{conf}(x)$  describes our model of confinement [2,3].

The  $T$  matrix in the  $q\bar{q}$  channel with the quantum numbers of the rho is

$$T_\rho(q^2) = \frac{G_\rho}{1 - G_\rho [\hat{J}_\rho(q^2) + \hat{K}_\rho(q^2)]} \quad , \tag{2.7}$$

if we neglect reference to Dirac and isospin matrices. (By expanding the denominator in Eq. (2.7), one can understand which diagrams are summed to obtain the  $T$  matrix.) We may introduce the rho meson into the formalism by writing

$$\frac{G_\rho}{1 - G_\rho [\hat{J}_\rho(q^2) + \hat{K}_\rho(q^2)]} = - \frac{g_{\rho qq}^2(q^2)}{q^2 - m_\rho^2 + im_\rho \Gamma_\rho(q^2)} \quad . \tag{2.8}$$

Equation (2.8) may be taken as the definition of the momentum-dependent rho-quark coupling parameter,  $g_{\rho qq}(q^2)$ . [See Table 1.] The mass of the rho is obtained from the equation

$$1 - G_\rho [\hat{J}_\rho(m_\rho^2) + \text{Re} \hat{K}_\rho(m_\rho^2)] = 0 \quad . \tag{2.9}$$

(In practice  $G_\rho$  is varied so that the rho mass is given correctly.) It may be seen that

$$m_\rho \Gamma_\rho(q^2) = g_{\rho qq}^2(q^2) \text{Im} K_\rho(q^2) \quad , \tag{2.10}$$

a relation which has a straightforward diagrammatic representation. We use the notation  $g_{\rho qq} = g_{\rho qq}(m_\rho^2)$ , etc. Quite similar relations may be written for the omega meson, thereby defining  $g_{\omega qq}(q^2)$  and  $g_{\omega qq} = g_{\omega qq}(m_\omega^2)$ , etc. Values obtained for  $g_{\rho qq}(q^2)$  and  $g_{\omega qq}(q^2)$  in our previous work [9] are presented in Table 1.

In our work we also found it useful to define momentum-dependent meson decay parameters,  $g^\rho(q^2)$  and  $g^\omega(q^2)$ . The meson decay constants,  $g^\rho = g^\rho(m_\rho^2)$  and  $g^\omega = g^\omega(m_\omega^2)$ , have values of (approximately)  $g^\rho = 5.05$  and  $g^\omega = 17.0$ . There are several different notations used in the literature for the meson decay constants. For example, in our notation, we have for the decay  $\rho^0 \rightarrow e^+ + e^-$ ,

$$\Gamma_{\rho^0 \rightarrow e^+ e^-} = \frac{4\pi\alpha^2}{3} \left[ \frac{1}{g^\rho} \right]^2 m_\rho, \quad (2.11)$$

with  $1/g^\rho = 0.198 \pm 0.009$ . Therefore, we use  $g^\rho = 5.05$  in our analysis. In a similar fashion, we find  $g^\omega = 17.0$ . In our analysis of the VMD model, we found the relation [6]

$$\frac{m_\rho^2}{g^\rho(q^2)} = \frac{g_{\rho qq}(q^2)}{2G_\rho}, \quad (2.12)$$

$$= \frac{g_{\rho qq}(q^2)}{2} \left[ \hat{j}_{(\rho)}(m_\rho^2) + \text{Re} \hat{K}_{(\rho)}(m_\rho^2) \right], \quad (2.13)$$

where we have used Eq. (2.9) to pass from Eq. (2.12) to Eq. (2.13). Also, we had [6]

$$\frac{m_\omega^2}{g^\omega(q^2)} = \frac{g_{\omega qq}(q^2)}{6G_\omega}, \quad (2.14)$$

$$= \frac{g_{\omega qq}(q^2)}{6} \left[ \hat{j}_{(\omega)}(m_\omega^2) + \text{Re} \hat{K}_{(\omega)}(m_\omega^2) \right]. \quad (2.15)$$

### III. The Pion Electromagnetic Form Factor

In an earlier work [1] we found the following expression for the contributions of the diagrams of Fig. 3a and 3b to the pion electromagnetic form factor,

$$F_{\pi}^{(1)}(q^2) = \left\{ -\frac{m_{\rho}^2}{g^{\rho}(q^2)} - \frac{m_{\omega}^2}{g^{\omega}(q^2)} \left[ \frac{1}{q^2 - m_{\omega}^2 + im_{\omega}\Gamma_{\omega}(q^2)} \right] \Theta_{(\omega\rho)}(q^2) \right. \\ \left. \times \left[ \frac{1}{q^2 - m_{\rho}^2 + im_{\rho}\Gamma_{\rho}(q^2)} \right] g_{\rho\pi\pi}(q^2) \right\}, \quad (3.1)$$

where

$$\Theta_{(\omega\rho)}(q^2) = -g_{\omega\pi\pi}(q^2)\hat{J}_{(\omega\rho)}(q^2)g_{\rho qq}(q^2) + e^2 \frac{m_{\omega}^2}{g^{\omega}(q^2)} \frac{m_{\rho}^2}{g^{\rho}(q^2)} \frac{1}{q^2}. \quad (3.2)$$

We have now included the electromagnetic process shown in Fig. 3e in the definition of  $\Theta_{(\omega\rho)}(q^2)$ . We may identify  $\Theta_{(\omega\rho)}(m_{\omega}^2) = \langle \rho^0 | H_{SB} | \omega \rangle$ , where  $\langle \rho^0 | H_{SB} | \omega \rangle$  is the matrix element introduced earlier. We note that the two terms in Eq. (3.2) have the opposite sign. We now add the direct omega decay to define

$$F_{\pi}(q^2) = F_{\pi}^{(1)}(q^2) + F_{\pi}^{(2)}(q^2) \quad (3.3)$$

where

$$F_{\pi}^{(2)}(q^2) = -\frac{m_{\omega}^2}{g^{\omega}(q^2)} \frac{1}{q^2 - m_{\omega}^2 + im_{\omega}\Gamma_{\omega}(q^2)} g_{\omega\pi\pi}(q^2). \quad (3.4)$$

In our analysis we make the following approximations. We use empirical (constant) values for  $g^{\rho}(q^2)$  and  $g^{\omega}(q^2)$ . (We choose  $g^{\rho} = 5.05$  and  $g^{\omega} = 17.0$ .) For  $\Gamma_{\rho}(q^2)$  we use the approximation



$$\Gamma_\rho(q^2) = \Gamma_\rho \left[ \frac{q^2 - 4m_\pi^2}{m_\rho^2 - 4m_\pi^2} \right] \quad (3.5)$$

which reproduces our results for  $\Gamma_\rho(q^2)$  presented in Fig. 2 quite well. Although, we include some  $q^2$  dependence of  $g_{\rho\pi\pi}(q^2)$  in our calculations, we find that it is a quite small effect. [See Table 1.] We also find that it is sufficient to take  $\Theta_{(\omega\rho)}(q^2) = \Theta_{(\omega\rho)}(m_\omega^2)$  and to put  $\Gamma_\omega(q^2) = \Gamma_\omega(m_\omega^2) = 8.4$  MeV.

It is clear that the importance of direct omega decay depends upon the value of  $g_{\omega\pi\pi}(m_\omega^2)$ . The calculations described in the following section yield  $g_{\omega\pi\pi}(m_\omega^2) = 0.0236$ , when  $\Delta m = m_d^0 - m_u^0 = 3.0$  MeV.

#### IV. Calculation of $g_{\rho\pi\pi}(q^2)$ and $g_{\omega\pi\pi}(q^2)$

It is useful to define a  $\rho\pi\pi$  vertex with reference to Fig. 4a,

$$\mathcal{F}_{\pi\pi}^\mu(q, \kappa) = (-1)2n_c I_f g_{\pi qq}(m_\pi^2) \int \frac{d^4k}{(2\pi)^4} \text{Tr} \left[ \Gamma^\mu(q, k) iS(-q/2 + k) \gamma_5 \right. \\ \left. \times iS(k - \kappa) \gamma_5 iS(q/2 + k) \right] , \quad (4.1)$$

$$= 2\hat{k}^\mu F_{\pi\pi}(q^2) , \quad (4.2)$$

where  $n_c = 3$  and  $I_f = -2$  has its origin in an isospin trace. Here  $S(k) = [k - m + i\epsilon]^{-1}$ . We write

$$F_{\pi\pi}(q^2) = -I_f n_c g_{\pi qq}^2(m_\pi^2) H(q^2) , \quad (4.3)$$

thereby defining  $H(q^2)$ . (Note that  $F_{\pi\pi}(q^2)$  and  $H(q^2)$  are real and negative. See Fig. 5.)

We also see that we may put

$$g_{\rho\pi\pi}(q^2) = -g_{\rho qq}(q^2)F_{\pi\pi}(q^2) . \quad (4.4)$$

We are interested in calculating  $g_{\omega\pi\pi}(q^2)$ . That may be done by generalizing the above calculation made for  $g_{\rho\pi\pi}(q^2)$ . For example, we may consider unequal constituent masses,  $m_u \neq m_d$ . We then write

$$H_{(\rho)}(q^2) = \frac{1}{2} \left[ H(m_u, m_d, m_u, q^2) + H(m_d, m_u, m_d, q^2) \right] , \quad (4.5)$$

with reference to Fig. 4b. That is, the up and down quark propagators in Eq. (4.1) have different masses. [See Fig. 4b.] We now define the integral governing omega decay,

$$H_{(\omega)}(q^2) = \frac{1}{2} \left[ H(m_u, m_d, m_u, q^2) - H(m_d, m_u, m_d, q^2) \right] . \quad (4.6)$$

[See Fig. 5.] Note the minus sign in Eq. (4.6) relative to Eq. (4.5). The calculation is most easily made by taking  $m = (m_u + m_d)/2 = 260$  MeV,  $m_u = 250$  MeV and  $m_d = 270$  MeV. The result for  $H_{(\omega)}(q^2)$  is proportional to  $\Delta m = m_d - m_u = m_d^0 - m_u^0$ . Therefore, to obtain the value of  $H_{(\omega)}(q^2)$  for a particular value of  $\Delta m$ , we multiply the value calculated for  $m_u = 250$  MeV and  $m_d = 270$  MeV by  $(\Delta m/20)$  where  $\Delta m$  is in MeV units. For our calculations we take  $\Delta m = 3$  MeV, a value consistent with the final results of our study. From Eq. (4.3), we see that

$$\frac{g_{\omega\pi\pi}(q^2)}{g_{\rho\pi\pi}(q^2)} = \frac{g_{\omega qq}(q^2)}{g_{\rho qq}(q^2)} \frac{H_{(\omega)}(q^2)}{H_{(\rho)}(q^2)} . \quad (4.7)$$

Note that  $g_{\omega qq}(m_\omega^2) = 2.95$  and  $g_{\rho qq}(m_\omega^2) = 2.80$ . [See Table 1.] We find  $g_{\omega\pi\pi}(m_\omega^2) = 0.0236$  and  $g_{\rho\pi\pi}(m_\rho^2) = 5.90$ , so that

$$g_{\rho\pi\pi}(m_\omega^2)/g_{\rho\pi\pi}(m_\omega^2) \approx 4 \times 10^{-3} . \quad (4.8)$$

It is this very small ratio that makes direct omega decay a relatively unimportant correction in the calculation of rho-omega mixing for the pion electromagnetic form factor.

## V. Results of Numerical Calculation for the Form Factor

In Fig. 7 we show our results for  $\Gamma_\rho = 144$  MeV. [See Fig. 2.] The dashed line represents  $|F_\pi^{(1)}(s)|^2$ , while the solid line represents  $|F_\pi(s)|^2$  of Eq. (3.3). The calculation was made for  $\Theta_{(\omega\rho)}(m_\omega^2) = -5033$  MeV<sup>2</sup>. (Actually, what is determined is  $\Theta_{(\omega\rho)}(m_\omega^2)/g^\omega = -296.1$  MeV<sup>2</sup>, so that, for  $g^\omega = 17.0$ , we have the value quoted,  $\Theta_{(\omega\rho)}(m_\omega^2) = -5033$  MeV<sup>2</sup>.) Since the electromagnetic term of Eq. (3.2) has the value 633 MeV, the strong mixing element is  $\Theta_{(\omega\rho)}^{st}(m_\omega^2) = (-5666 \pm 600)$  MeV<sup>2</sup>, where we have added a conservative estimate of the error expected in this procedure.

The results are rather sensitive to the value of  $\Gamma_\rho$ . For example, in Fig. 8 we show another result obtained when fitting the data. While  $\Gamma_\rho = 144$  MeV was used for Fig. 7, we use  $\Gamma_\rho = 147$  MeV for the results shown in Fig. 8. We see that the theoretical values for  $\sqrt{s} < 0.77$  MeV have been improved somewhat, at the cost of a somewhat poorer fit in the region  $\sqrt{s} > 0.77$  MeV. (Compare Figs. 7 and 8.)

## VI. Discussion

One of the more interesting aspects of our calculation is the relation we have found between  $\Delta m = m_d^0 - m_u^0$  and the value of  $\Theta_{(\omega\rho)}^{st} \equiv \Theta_{(\omega\rho)}^{st}(m_\omega^2)$ . In our earlier work [6], we had  $\Delta m = 2.67 \pm 0.3$  MeV, if we used a calculation of  $\hat{J}_{(\rho\omega)}(q^2)$  that gave  $\hat{J}_{(\rho\omega)}(0) = 0$ . However,

that value for  $\Delta m$  was given for the case  $g^\omega = 15.2$ . If we use the more recent value of  $g^\omega = 17.0$ , we have  $\Delta m = 3.0 \pm 0.3$  MeV.

If we are to obtain the correct value of the pion mass for the value of the momentum cutoff used in the NJL model ( $\Lambda_E = 1$  GeV), we need  $m_q^0 = (m_u^0 + m_d^0)/2 = 5.5$  MeV [11]. Thus, we find  $m_u^0 = 4$  MeV and  $m_d^0 = 7$  MeV, with  $m_u^0/m_d^0 \approx 0.57$  which is quite close to the value of  $m_u^0/m_d^0 \approx 0.55$  suggested by Weinberg [10].

### Acknowledgment

This work was supported in part by a grant from the National Science Foundation and by the PSC-CUNY Faculty Research Award Program of the City University of New York.

## References

- [1] C.M. Shakin and Wei-Dong Sun, Brooklyn College Report: BCCNT 95/101/251 (1995)  
– submitted for publication in Physical Review D.
- [2] L.S. Celenza, C.M. Shakin, Wei-Dong Sun, J. Szweda, and Xiquan Zhu, Ann. Phys. (N.Y.) 241, 1 (1995).
- [3] L.S. Celenza, C.M. Shakin, Wei-Dong Sun, J. Szweda, and Xiquan Zhu, Phys. Rev. D51, 3638 (1995).
- [4] An extensive review of  $\rho$ - $\omega$  mixing may be found in H.B. O'Connell, B.C. Pearce, A.W. Thomas, and A.G. Williams, to appear in Trends in Particle and Nuclear Physics, ed. W.Y. Pauchy Hwang (Plenum Press) hep-ph/9501251.
- See also,
- H.B. O'Connell, B.C. Pearce, A.W. Thomas, and A.G. Williams, Phys. Lett. B336, 1 (1994); *ibid.* B354, 14 (1995);
- T. Hatsuda, E.M. Henley, Th. Meissner, and G. Krein, Phys. Rev. C49, 452 (1994);
- K.L. Mitchell, P.C. Tandy, C.D. Roberts, and R.T. Cahill, Phys. Lett. B335, 282 (1994).
- R. Friedrich and H. Reinhardt, Nucl. Phys. A594, 406 (1995).
- [5] S.A. Coon and R.G. Barrett, Phys. Rev. C36, 2189 (1987).
- [6] Shun-fu Gao, C.M. Shakin, and Wei-Dong Sun, Brooklyn College Report: BCCNT 95/082/250R4 (1995) – to be published in Physical Review C (March, 1996).
- [7] Kim Maltman, H.B. O'Connell and A.G. Williams, University of Adelaide preprint: ADP-95-50/T197 (1996).

- [8] L.M. Barkov *et al.*, Nucl. Phys. B256 365 (1985).
- [9] Shun-fu Gao, C.M. Shakin, and Wei-Dong Sun, Brooklyn College Report: BCCNT 95/032/245R1 (1995) – unpublished.
- [10] S. Weinberg, in Festschrift for I.I. Rabi, edited by L. Motz (New York Acad. Sci., New York, 1977).
- [11] Nan-Wei Cao, C.M. Shakin, and Wei-Dong Sun, Phys. Rev. C46, 2535 (1992).

Table 1. Values of  $g_{\rho qq}(q^2)$ ,  $g_{\omega qq}(q^2)$  and  $g_{\rho\pi\pi}(q^2)$  are given [9].

$q^2$ (GeV <sup>2</sup> )	$g_{\rho qq}(q^2)$	$g_{\omega qq}(q^2)$	$g_{\rho\pi\pi}(q^2)$
0.7	2.66	2.80	5.85
0.6	2.82	2.98	5.90
0.5	2.98	3.14	5.93
0.4	3.13	3.30	6.05
0.3	3.27	3.45	6.25
0.2	3.41	3.59	6.45
0.1	3.54	3.73	6.60
0.0	3.66	3.86	6.74
-0.1	3.74	3.96	6.81
-0.2	3.81	4.04	6.80
-0.3	3.88	4.11	6.79
-0.4	3.92	4.16	6.75
-0.5	3.97	4.21	6.70
-0.6	4.01	4.25	6.65
-0.7	4.04	4.29	6.55
-0.8	4.07	4.32	6.45
-0.9	4.10	4.35	6.32
-1.0	4.12	4.38	6.20



### Figure Captions

Fig. 1. Diagrammatic elements appearing in the calculation of isovector, isoscalar and mixing polarization tensors.

- (a) A contribution to the isovector polarization tensor is shown. If  $m_d^0 = m_u^0$ , we have  $\hat{J}_{(\rho)}^{\mu\nu}(q) = \hat{J}_{(\omega)}^{\mu\nu}(q)$ . The solid lines denote quarks and the shaded area denotes a vertex of a confining potential.
- (b) Coupling to the two-pion continuum serves to define a polarization tensor,  $\hat{K}_{(\rho)}^{\mu\nu}(q)$ .
- (c) The polarization tensor  $\hat{J}_{(\rho\omega)}^{\mu\nu}(q)$  that describes rho-omega mixing. This tensor is calculated as the difference of two integrals. The first has a constituent quark mass of  $m = m_u$ , while the second has  $m = m_d$ . (Note that  $m_u - m_d = m_u^0 - m_d^0$  in the NJL model, so that  $\hat{J}_{(\rho\omega)}^{\mu\nu}(q) = 0$ , if  $m_u^0 = m_d^0$ .)

Fig. 2. Calculated values of the momentum dependent rho width are shown. (The relation  $m_\rho \Gamma_\rho(s) = g_{\rho qq}^2(s) \text{Im} K_{(\rho)}(s)$  of Eq. (2.10) is used.) the calculated values are well approximated by

$$\Gamma_\rho(s) = 144 \left[ \frac{s - 4m_\pi^2}{m_\rho^2 - 4m_\pi^2} \right] \text{MeV}.$$

Fig. 3. A vector meson dominance model for the pion electromagnetic form factor is shown.

- (a) Rho-dominance of the form factor is depicted. The photon is denoted by a dashed line.
- (b) Contribution to the form factor due to omega-rho mixing. The calculation requires knowledge of the tensor  $J_{(\rho\omega)}^{\mu\nu}(q)$  of Fig. 1c.

- (c) Contribution of direct omega decay to the pion electromagnetic form factor.
- (d) A contribution to the pion form factor. This term is very small and is neglected.
- (e) The electromagnetic term that contributes to  $\Theta_{(\rho\omega)}(q^2)$  is shown. Here the dashed lines are photons. [See Eq. (3.2).]

Fig. 4. Form factors for meson decay to two pions are shown.

- (a) If  $m_u^0 = m_d^0$ , we define a form factor  $\mathcal{F}_{\pi\pi}^\mu(q, \kappa)$  that is proportional to  $H(q^2)$ . [See Eqs. (4.2) and (4.3).]

- (b) If  $m_u^0 \neq m_d^0$ , the rho-pion form factor  $\mathcal{F}_{\rho\pi\pi}^\mu(q, \kappa)$  proportional to the quantity
 
$$\frac{1}{2} \left[ H(m_u, m_d, m_u, q^2) + H(m_d, m_u, m_d, q^2) \right].$$

[See Fig. 5.]

- (c) If  $m_u^0 \neq m_d^0$ , the omega-pion form factor is proportional to the quantity

$$\frac{1}{2} \left[ H(m_u, m_d, m_u, q^2) - H(m_d, m_u, m_d, q^2) \right].$$

[See Fig. 5.]

Fig. 5. The figure shows the values of  $H(q^2)$  as a solid line. The calculation is made for  $m_d = m_u = 260$  MeV. The dotted line represents  $H(m_u, m_d, m_u, q^2)$  and is calculated for  $m_u = 250$  MeV and  $m_d = 270$  MeV. The dashed line represents  $H(m_d, m_u, m_d, q^2)$  and is also calculated for  $m_u = 250$  MeV and  $m_d = 270$  MeV. (Values for the case  $m_u = 260$  MeV and  $m_d = 263$  MeV may be obtained from these results, since  $H(m_u, m_d, m_u, q^2)$  and  $H(m_d, m_u, m_d, q^2)$  depend linearly on  $m_d^0 - m_u^0 = m_d - m_u$ .)

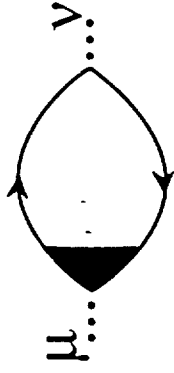
Fig. 6. The dotted line shows the values of  $|F_\pi(s)|^2$  in the rho-dominance model of Fig. 3a. (The calculation is made for  $\Gamma_\rho(s)$  shown in Fig. 2, where  $\Gamma_\rho = 144$  MeV.)

The solid line includes the effect of  $\rho$ - $\omega$  mixing as depicted in Fig. 3b. Here  $g^\rho = 5.05$ ,  $g^\omega = 17.0$  and  $\Theta_{(\rho\omega)} = -5033 \text{ MeV}^2$ .

Fig. 7. The dashed line shows  $|F_\pi(s)|^2$  in the rho-dominance model. (See Fig. 6.) The solid line includes the effect of  $\rho$ - $\omega$  mixing as shown in Fig. 3b. The dotted line includes the effects of both rho-omega mixing and direct omega decay, as depicted in Fig. 3c. Here  $\Gamma_\rho(s) = 144(s - 4m_\pi^2)/(m_\rho^2 - 4m_\pi^2) \text{ MeV}$  was used, with  $g^\rho = 5.05$ ,  $g^\omega = 17.0$ ,  $\Theta_{(\rho\omega)} = -5033 \text{ MeV}^2$  and  $g_{\omega\pi\pi}(m_\omega^2) = 0.0236$ .

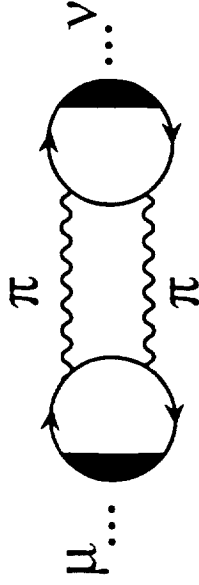
Fig. 8. Same caption as Fig. 7, except that  $\Gamma_\rho(s) = 147(s - 4m_\pi^2)/(m_\rho^2 - 4m_\pi^2) \text{ MeV}$  was used in the calculation.

$$-i\hat{J}_{(p)}^{\mu\nu}(q)$$



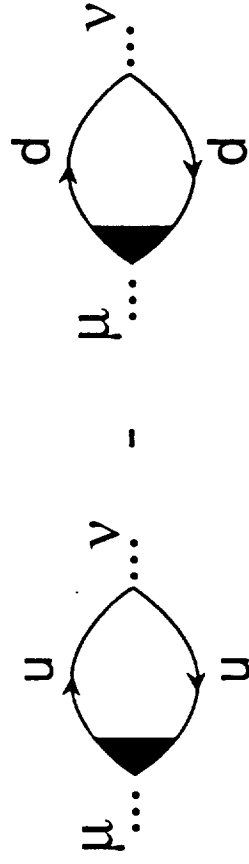
(a)

$$-i\hat{K}_{(p)}^{\mu\nu}(q)$$



(b)

$$-i\hat{J}_{(p\omega)}^{\mu\nu}(q)$$



(c)

FIG. 1

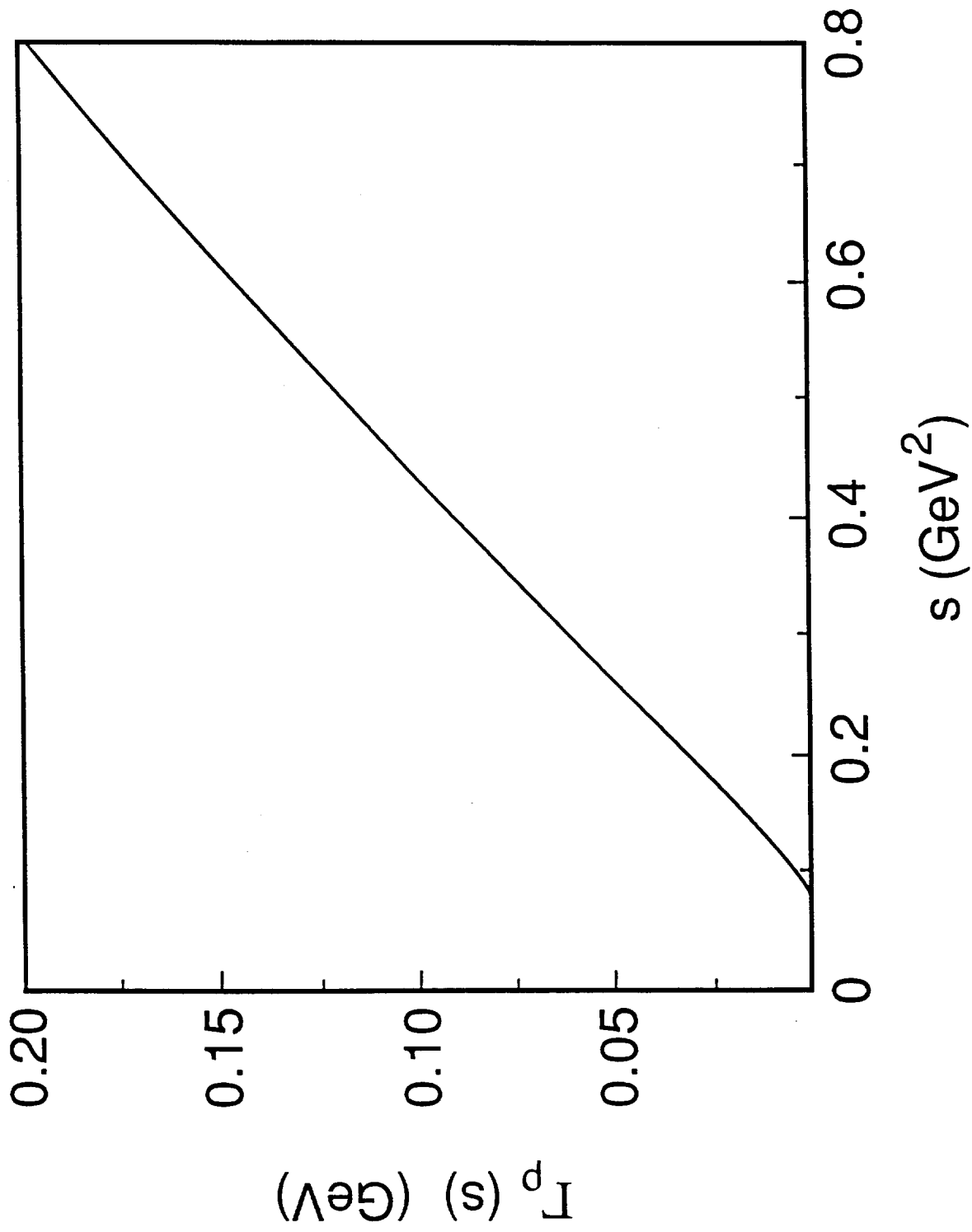
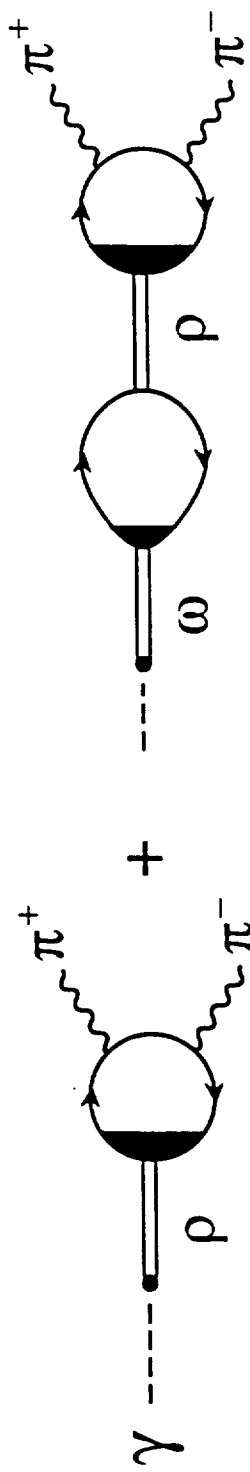
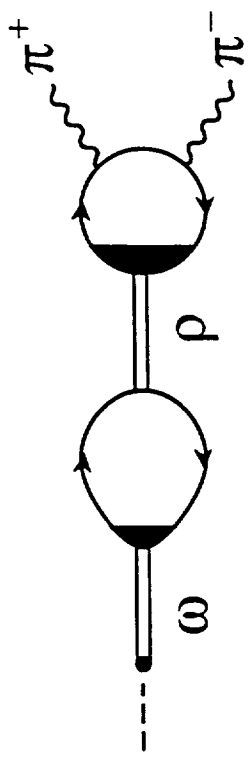


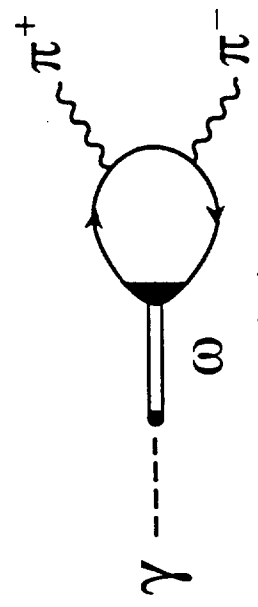
FIG. 2



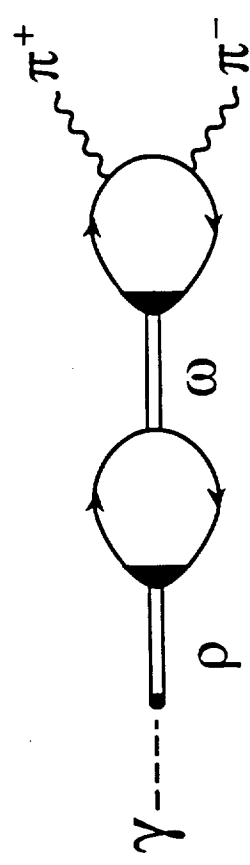
(a)



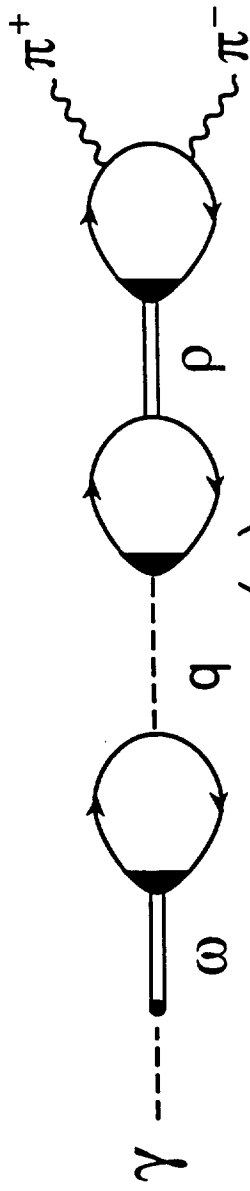
(b)



(c)



(d)



(e)

FIG. 3

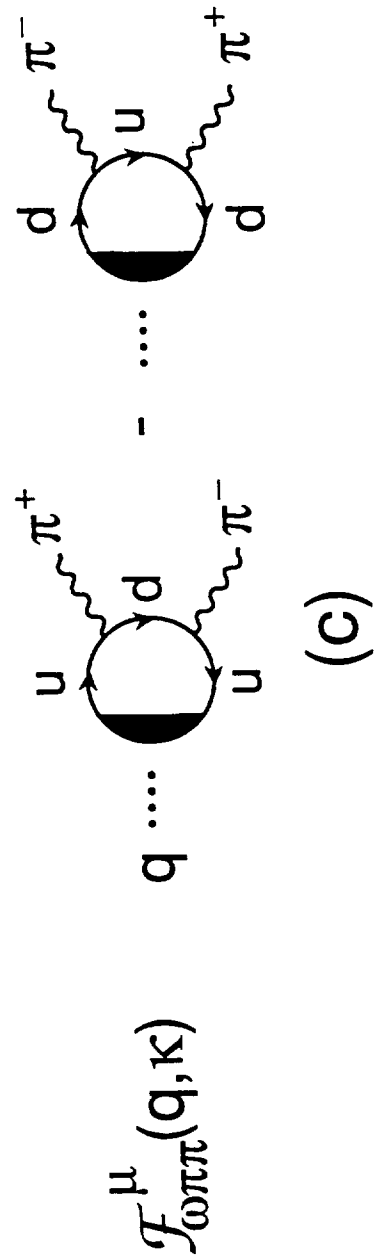
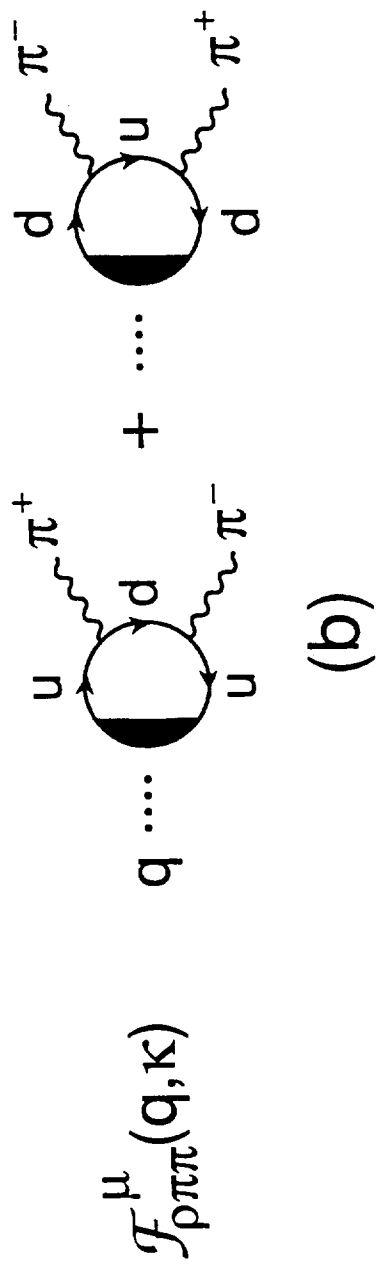
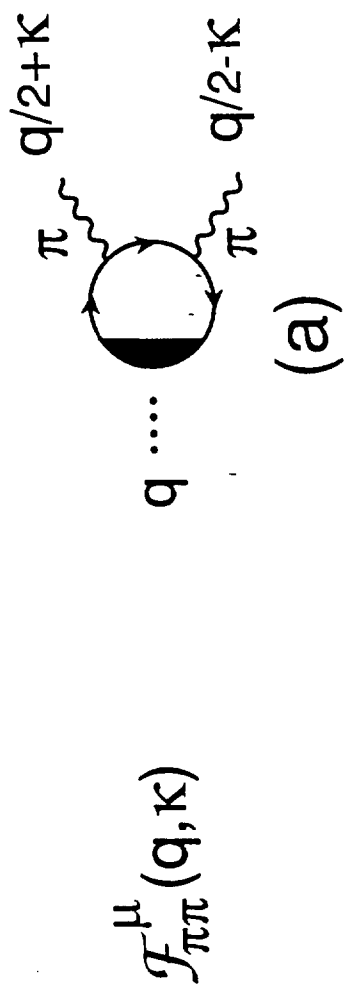


FIG. 4

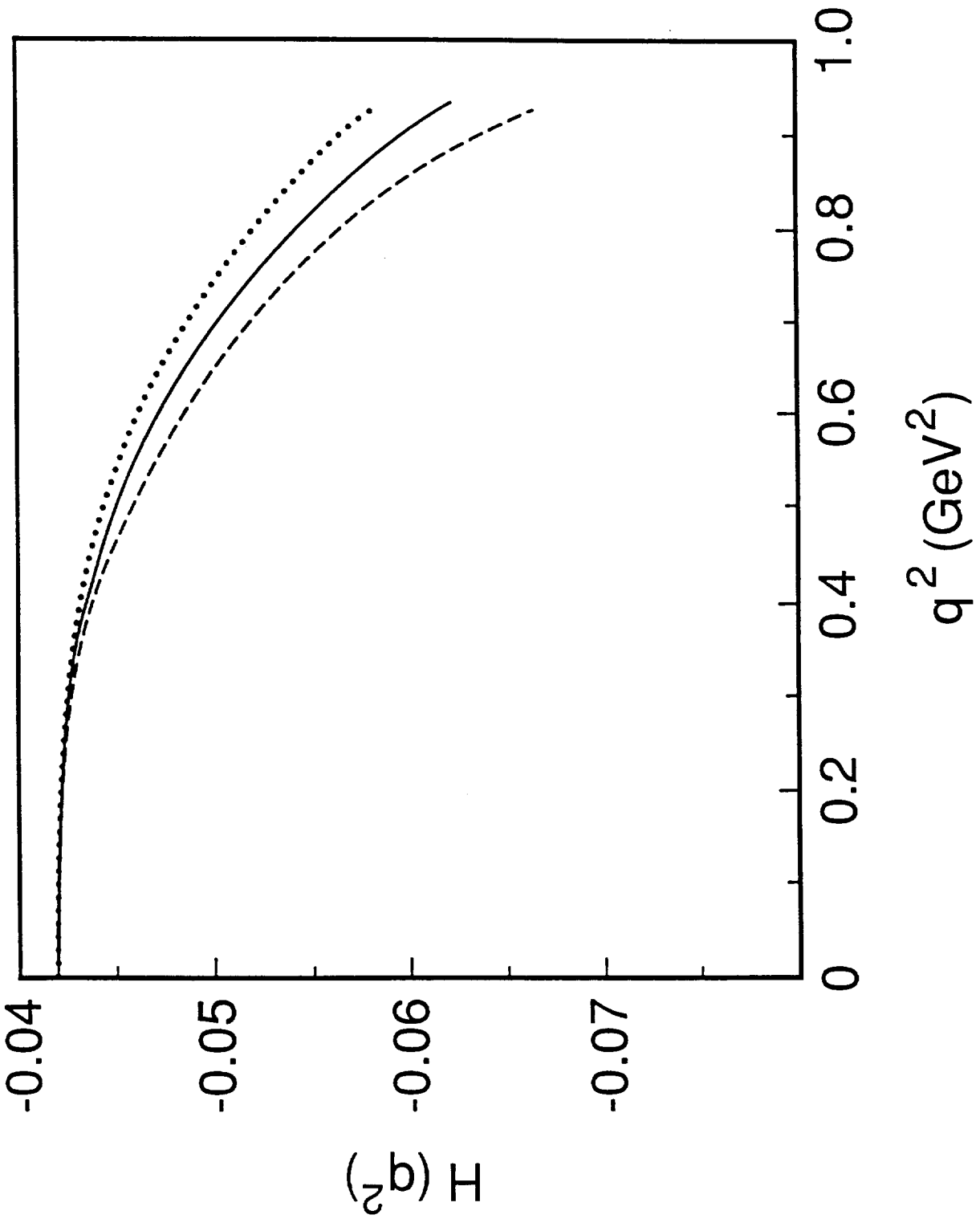


FIG. 5



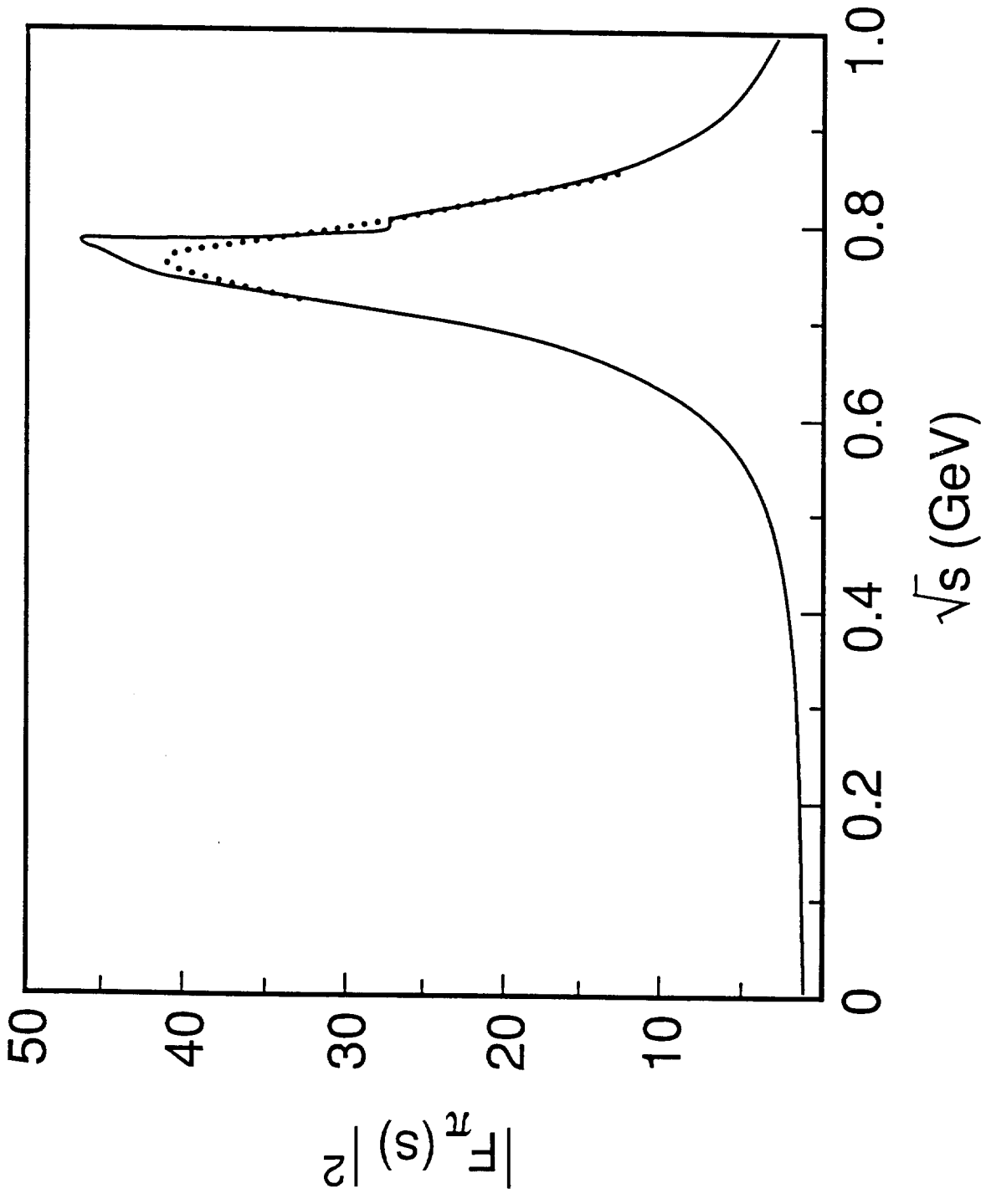


FIG. 6

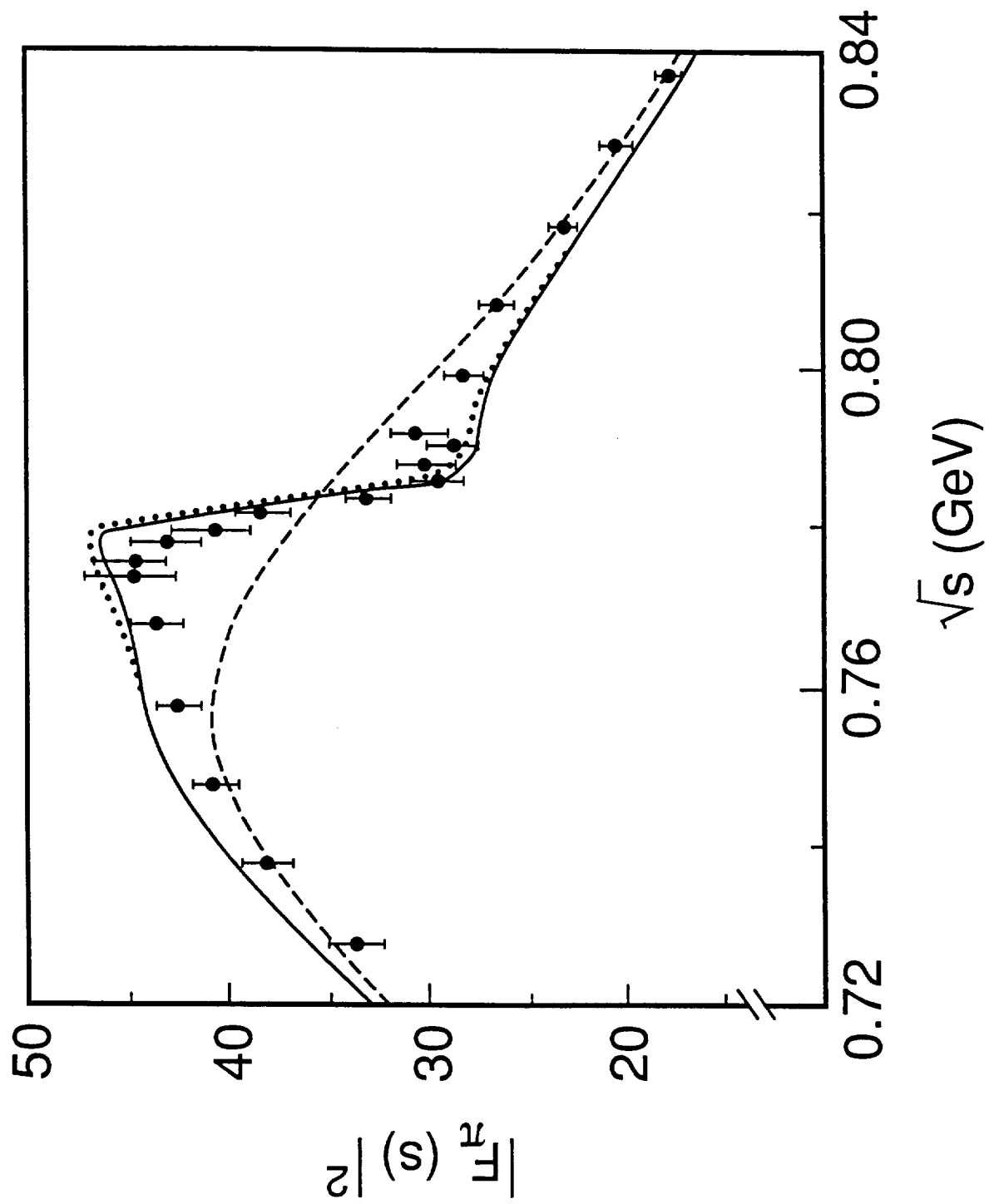


FIG. 7

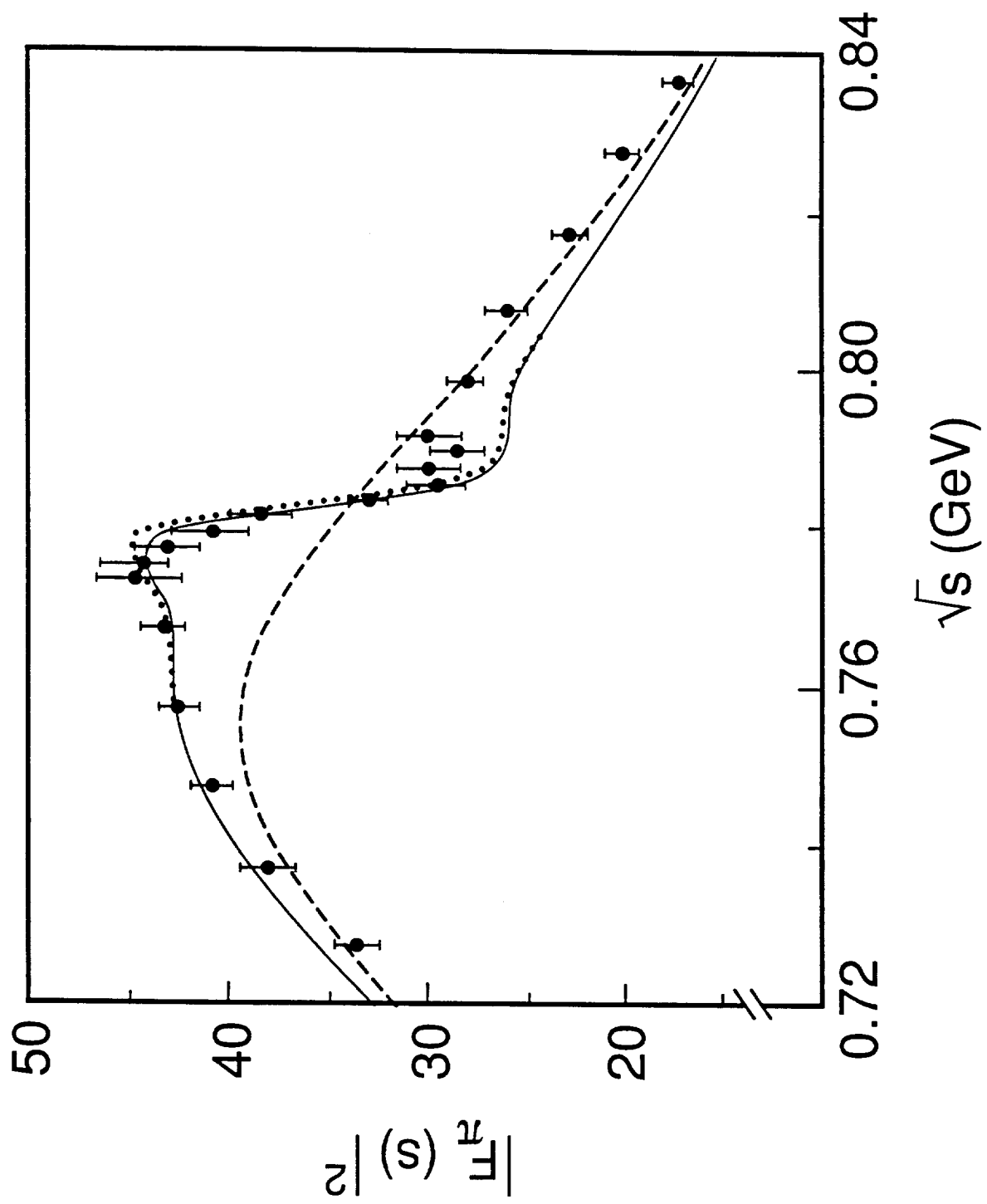


FIG. 8

•  
•  
•  
•  
•

